Possible Organization for Writing a Thesis including a LaTeXFramework and
Examples

by

Mohammad Ghasemiahmadi
B.Sc., University of Terhan, 2015

A Dissertation Submitted in Partial Fulfillment of the
Requirements for the Degree of

MASTER OF APPLIED SCIENCE

in the Department of Electrical and Computer Engineering

© Mohammad Ghasemiahmadi, 2017
University of Victoria

Possible Organization for Writing a Thesis including a LaTeX Framework and Examples

by

Mohammad Ghasemiahmadi
B.Sc., University of Terhan, 2015

Supervisory Committee

Dr. Lin Cai, Supervisor
(Department of Electrical and Computer Engineering)

Dr. M. Member One, Departmental Member
(Department of Same As Candidate)

Dr. Member Two, Departmental Member
(Department of Same As Candidate)

Dr. Outside Member, Outside Member
(Department of Not Same As Candidate)

Supervisory Committee

Dr. Lin Cai, Supervisor
(Department of Electrical and Computer Engineering)

Dr. M. Member One, Departmental Member
(Department of Same As Candidate)

Dr. Member Two, Departmental Member
(Department of Same As Candidate)

Dr. Outside Member, Outside Member
(Department of Not Same As Candidate)

ABSTRACT

This document is a possible Latex framework for a thesis or dissertation at UVic. It should work in the Windows, Mac and Unix environments. The content is based on the experience of one supervisor and graduate advisor. It explains the organization that can help write a thesis, especially in a scientific environment where the research contains experimental results as well. There is no claim that this is the *best* or *only* way to structure such a document. Yet in the majority of cases it serves extremely well as a sound basis which can be customized according to the requirements of the members of the supervisory committee and the topic of research. Additionally some examples on using LaTeX are included as a bonus for beginners.

Contents

List of Tables

List of Figures

ACKNOWLEDGEMENTS

I would like to thank:

my cat, Star Trek, and the weather, for supporting me in the low moments.

Lin Cai, for mentoring, support, encouragement, and patience.

Grant Organization Name, for funding me with a Scholarship.

I believe I know the only cure, which is to make one's centre of life inside of one's self, not selfishly or excludingly, but with a kind of unassailable serenity-to decorate one's inner house so richly that one is content there, glad to welcome any one who wants to come and stay, but happy all the same in the hours when one is inevitably alone.

Edith Wharton

DEDICATION

I dedicate this work to my family. My parents, who I wouldn't be where I am if I didn't have their support. My better half, Ghazale, who's always been there for me.

Chapter 1

Introduction

The word *IoT*, which stands for Internet of Things, describes an environment where every "*thing*" is connected to the Internet. The use of the word "*thing*" suggests that no device is exempt. The number of opportunities that a world where every device, small or large is connected to a global network brings, is beyond anyone's imagination. As always, along with opportunities come challenges that need to be resolved for such a scenario to function properly. Almost all layers of communication protocol need to be redesigned to handle these challenges, together with an effort to come up with applications that can use the extra-connectivity in its full potential.

1.1 My Claims

Something must be new in this work, no matter how small, since you are getting a graduate degree for it! Tell me about it clearly and succintly right now, just as you did in the abstract. Make an impact here. How about something like the following box:

I make *four* claims which my dissertation validates:

> My new algorithm to solve the problem of doing nothing include these important new features whose practical applicability can be proved both formally and empirically:
>
> 1. first feature;
>
> 2. second feature;
>
> 3. everything is much easier to understand, and therefore, easier to implement correctly.

Claim 1 and claim 2 are *quantitative* - they will be proven by experiment.
Claim 3 is *qualitative* - they will be demonstrated by argument.

1.1.1   The Importance of My Claims

Some very important positive consequences arise from the validation of the above claims. It is these consequences that comprise a significant positive contribution to research in the field of whatever the field is.

Claim 1 implies that:

1. Something profound which applies to:

   - something excellent;

   - something important.

2. Something else just as profound.

Claim 2 implies that:

- Repeat as above if necessary and useful.

The consequence of claim 3 is that:

- There must be something good coming out of all this work!

1.2   Agenda

This section provides a map of the dissertation to show the reader where and how it validates the claims previously made. Here is where I am also presenting my own style of organization which may be totally different from what your supervisor thinks. However, trust me, this is a good solid beginning for a structure. Your supervisor may ask you to change it, but will still appreciate what you have! For each of the chapters below I also give a short summary of what the main focus should be and then I expand on it a bit within the chapter itself.

Chapter 1 give and introduction about the concept of IoT

Chapter 2 describes in details the open problem which is to be tackled together with its context

Chapter 3 explaines the rss-based grouping strategy

Chapter 4 is going to explain the pnc implementation

Chapter 5 is the pnc practical experiments with photos of usrps

Chapter 6 is the evaluation resutls of both works.

Chapter 7 is the conclution

The list above is not complete. Chapter 3 actually includes a lot more, as I could not resist placing in it a few LATEXexamples to help you along. This document is not a primer for LATEX, but there is no harm done in giving a little help.

Chapter 2

The Problem to be Solved

This is thesis is trying to solve two problems. For single hop transmissions, the hidden terminal problem in infrastructure-based IoT scenarios is considered. And for multi-hop transmissions, the implementation of a physical layer network coding system for long distance relay transmissions is the focus.

Chapter 3

Single Hop Transmission

This is chapter expalins the rss-grouping work.

There has been a massive increase in the number of nodes connected to an Access Point (AP) in a Wireless Local Area Network (WLAN) in recent years. Technologies such as Internet of Things (IoT), sensor networks and Machine Type Communication (MTC) are anticipated to bring an even larger number of nodes all contending to access the license-free Industrial, Scientific, and Medical (ISM) bandwidth. This is part of the reason that the next generation of IEEE 802.11 standards includes a new sub 1GHz bandwidth to ISM in order to cover the IoT traffic [?]. But the number of connections from both MTC and human devices increases so fast that using conventional IEEE 802.11 MAC protocol's Distributed Coordination Function (DCF) to handle such a large number of nodes results in a high collision probability and very low channel efficiency.

Research efforts have been put to make super dense IEEE 802.11 networks more efficient. In addition to physical layer solutions trying to make wireless communications more efficient and faster, a key issue is how to modify the DCF protocol in the MAC layer to achieve better resource utilization. For instance, [?] proposed a method to adjust the transmission opportunity according to collision probability. One promising solution is grouping users and limiting the competitions within the group, used in Group Synchronized Distributed Coordination Function in the IEEE 802.11ah standard [?]. It has been proved in [?] and [?] that grouping users and dedicating a Restricted Access Window (RAW) to each group increases the overall throughput in wireless networks. The work at [?] has also addressed the problem of super dense networks and proposed a grouping scheme based on transmission attempts to assign larger RAWs to crowder groups instead of having equally timed RAWs.

3.1   802.11ah Standrad

Explain what 802.11ah is.

The 802.11ah protocol is one of the recent standards by IEEE organization. This standard introduces many new concepts for the first time, including new designs for both physical and MAC layer. The 802.11ah standard has been designed with three use cases in mind, smart sensors, back-haul aggregation and extended range hotspot. In smart sensor use case, 802.11ah is designed to handle a very large number of nodes(up to 6000) connected to one access point. In the back-haul use case, an 802.11ah access point is designed to be used as an aggregator for wireless personal area network(WPAN) devices that use IEEE 802.15.4.g standard. WPAN(802.15.4g) devices have small transmission range and data rate, so in this case, 802.15.4g routers, gather data from 802.15.4g devices and send them to a single 802.11ah aggregator. In the extended hot-spot use case, 802.11ah access points can be used as cellular offloading candidates specially in outdoor environment where other .11 standards suffer from their short range.

3.1.1   Physical Layer of 802.11ah

In the Physical Layer(PHY), 802.11ah makes use of sub 1GHz license-exempt bands. This is the main physical layer difference between this standard and previous .11 standards. Also, 802.11ah mostly focuses on small bandwidths and does not allow ¿20 MHz bands. The use of smaller carrier frequency also gives 802.11ah a much larger transmission range compared to other .11 standards. In outdoor scenarios, using default transmission power(200mW), 1MHz channel and Modulation and Coding Scheme(MCS) 10, it can achieve a range as high as 1 km.

3.1.2   MAC layer of 802.11ah

In the MAC layer 802.11ah introduces may new concepts from frame formats to channel access and power management. In the main 802.11 standard, number of nodes that can be connected to one access point is limited to 2007. 802.11ah extends this range to 8191 nodes to support the smart sensor use case. Also to better support dense network scenarios, 802.11ah shortens the length of frame headers, control frames such as ACKs and periodically transmitted frames such as beacons. The main change in 802.11ah which is also the focus of this paper are changes in the channel access.

In order to handle the large contention between nodes in dense scenarios, 802.11ah divides all nodes connected the access point into different groups, each is then given a specified time window called Restricted Access Window(RAW) to use the channel while members of all other groups remain silent. This also divides the beacon period into multiple RAWs each dedicated to one group. This not only decreases the contention that one node experiences while using the wireless channel, also lets nodes save power by going to sleep in RAW that do not belong to them. It is left to the access point to decide whether or not to allow nodes to cross the RAW boundary just to finish an ongoing transmission(Cross Slot Boundary). This channel access mechanism is called Group Synchronized Distributed Coordination Function (GS-DCF) which is to be used instead of the traditional DCF.

3.2   The Hidden Terminal Problem

Explain what hidden terminal problem is.

The hidden terminal is a traditional problem in wireless communication. Is usually happens when a node falls outside of sensing area of another node but they are both trying to communicate with a same node. Figure 3.1 illustrates a general case for the hidden terminal problem. For example, if the node A, first start the transmission of a packet to node B, and sometime in the middle of their communication, node C also decides to transmit a packet to B, according to the CSMA/CA procedure it will first listen to the channel, an since it can not sense the transmission coming from A. it will find the channel ideal and initiate its transmission to B which will result in collision and loss of both packets of A and C. Wireless LAN in the infrastructure mode considering the up-link transmission, since every other node wants for transmit to the access point, are vulnerable to this problem.

The legacy solution for this problem is the use of Request To Send(RTS) and Clear To Send(CTS) messages. Using these messages, every node has to send an RTS to its receiver and wait to get a CTS before starting a transmission. In this way, although node C might not sense the RTS from node A, it will receive the CTS that B sends to A and know that the channel for B is going to be busy. The only chance of collision because of the hidden terminal then is during the transmission of the RTS message. Since the RTS is a small control message, collision probability will be reduced significantly.

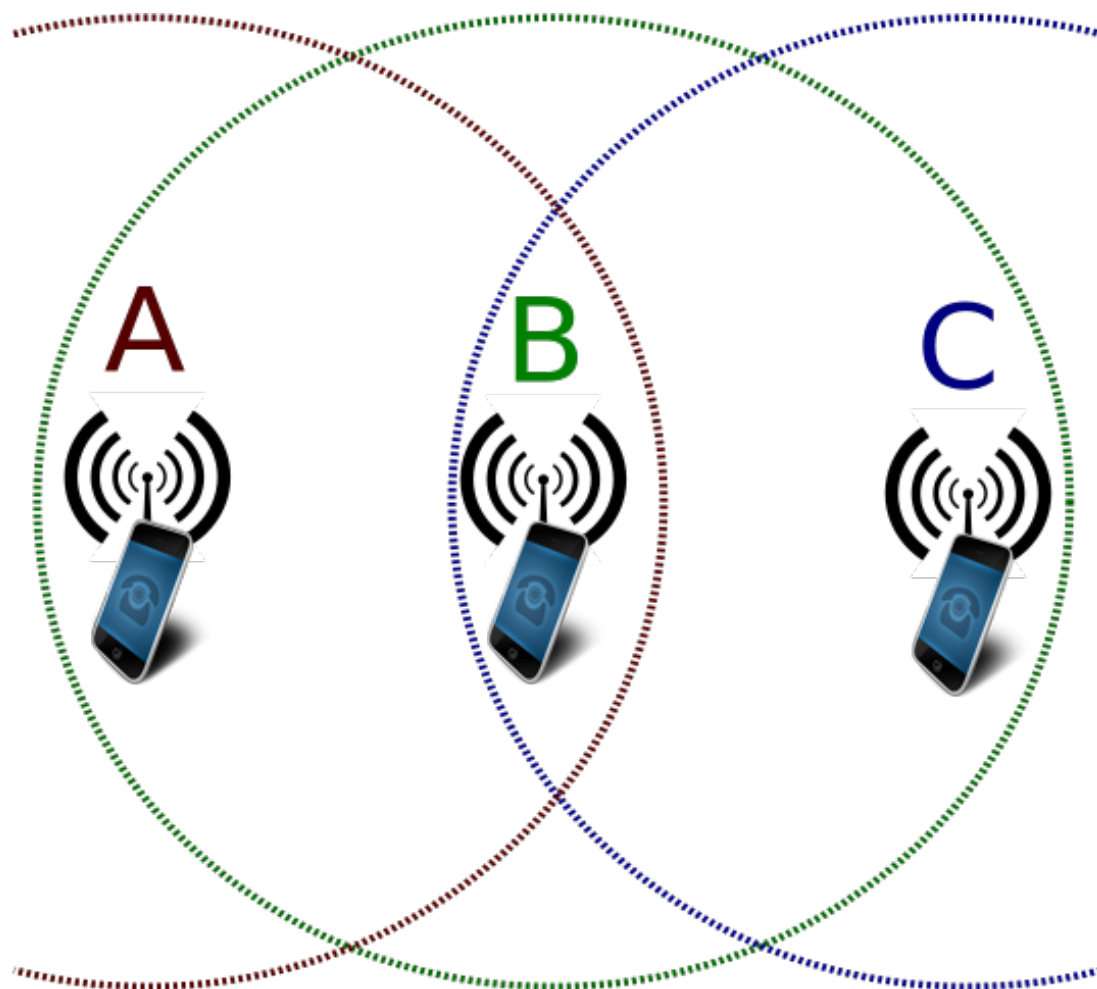Given the extended range of communication in the 802.11ah standard, this prob-

Figure 3.1: A simple hidden terminal problem

lem becomes even more serious.

3.3   Related Works

[?] has considered the hidden terminal with a new approach in a Constant Contention Window (CCW) scenario and studied the problem of two competing senders that cannot sense each other but are trying to transmit to a station that both can sense, a frequent situation in infrastructure mode networks.

One solution for the hidden terminal problem is using RTS/CTS mechanism. This mechanism solves the problem for the case that the transmission time of a data packet is much larger than that of RTS/CTS. However, it introduces additional overhead, and the collisions cannot be avoided due to the RTS packets from hidden terminals. In [?], the hidden terminal problem in GS-DCF based networks was discussed. The proposed hidden matrix based regrouping (HMR) algorithm can reduce the number of hidden terminals but it is a centralized approach and requires the access point to discover hidden terminal relationship between two nodes first and then solve it by regrouping one of them to another group.

The research in [?] has also studied the hidden terminal problem but in IEEE 802.15.4-based networks. A grouping mechanism similar to IEEE 802.11ah is proposed but the strategy to deal with the hidden terminal problem is still based on discovering hidden terminal relationships and rescheduling nodes.

[?] proposed a Group-based MAC where a new station join a group if the estimated distance to the group leader is below half of the transmission distance to avoid hidden-terminal, and otherwise a new group will be formed. The AP cannot effectively control the number of groups.

When the AP can obtain the global information about the location of all nodes, existing clustering algorithms such as k-means can be applied and the group designation is completely controlled by the AP in a way similar to centralized grouping schemes described in [?].

However, when the number of terminals is large, collecting global information significantly increases the overhead of feedback. Assigning all of the nodes to their groups results in a high control overhead especially when the network is dynamic.

3.4   Rss-Based Grouping Strategy

3.4.1   Motivation

Although using GS-DCF function proposed in IEEE 802.11ah can improve final throughput compared to conventional IEEE 802.11 protocols, there are still some open issues resulting from the new sub 1GHz license-exempt bands in IEEE 802.11ah. Utilizing carrier frequencies smaller than 1 GHz can increase network coverage up to 1 km. This large distance makes the well-known hidden terminal problem more serious. As shown in [**?**, **?**, **?**], the hidden terminal problem can lead to a substantial performance degradation in infrastructure-based networks.

Although RTS/CTS and centralized grouping strategy have been proposed to address the hidden terminal problem [**?**, **?**], they are not suitable for IoT scenarios with small packet size and large number of nodes.

Based on the grouping idea in the IEEE 802.11ah standard, this chapter aims to solve the problem in a distributed manner without using RTS/CTS. Our solution ensures that nodes in the same group are close enough to each other so that they can always sense each other's transmission in their own RAW.

Different from the previous approaches, this thesis proposes an RSS-based grouping scheme. Nodes sense the received power from other nodes and join the group that has the largest sensed power. To the best of our knowledge, this is the first work to explicitly use signal strength for assigning nodes to their groups. The performance gain of the proposed method is then evaluated by analytical model and simulations. The main contributions of this paper are three-fold. First, we propose an RSS-based grouping strategy to solve the hidden terminal problem in IEEE 802.11ah networks. Second, we derive the probability of two nodes in one group being able to sense each other. Third, extensive simulations using NS-2[**?**] have been conducted, and the results show that, by using the proposed method, the hidden terminal problem becomes negligible in IEEE 802.11ah networks and RTS/CTS is no longer needed.

3.4.2   System Model

In this work, we consider an infrastructure based IEEE 802.11ah network, where each wireless terminal transmits its packets directly to the access point. The network coverage area is a circle with radius R where the access point is at the center. Nodes are uniformly distributed in the circle and their locations follow a Poisson Point

Process (PPP) with density λ. The latter two assumptions are used for analysis and they are not necessary for the algorithm to perform. Nodes are assumed to be static at their position which is a reasonable assumption for most IoT and sensor networks and an active node always has a packet to transmit.

The channel model used in the analysis is a pathloss model with parameters α and β in a way that the received power at a distance d from the transmitter node is

$$P_r(d) = \frac{\beta}{d^\alpha} P_t, \tag{3.1}$$

where P_t is transmit power. In the simulation, we also consider the Rayleigh fast-fading and log-normal shadowing model where the received power is an exponential random variable and its mean $\bar{\gamma}$ is a log-normal random variable as

$$\bar{\gamma}_{dB} = \mathcal{N}(10\log_{10}(P_r(d)), \sigma). \tag{3.2}$$

We refer to both centralized and distributed schemes used in [?] as random grouping schemes. We also do not distinguish between RAW slot crossing and not crossing cases known as CR-GS-DCF and NCR-GS-DCF respectively which has negligible impact on the grouping decision [?].

3.4.3   RSS-Based Grouping

In order to avoid disadvantages of a centralized solution mentioned before, one can utilize the idea of measuring the sensed power from other nodes to let users choose their own groups based on which group their neighbors are in. Here we propose a grouping scheme based on sensed power from other nodes. The grouping mechanism should be triggered by the access point (AP) using its Beacon Frame (BF) at each Grouping Update Period (GUP) and nodes should listen to the channel for the sensed power of pilot messages from group heads. Such a BF at the beginning of a GUP is called a Beacon* and its difference with conventional beacon frames is that there is a grouping procedure at its beginning.

We propose an RSS-based strategy that a node will listen to some pilot messages from randomly chosen nodes in a reserved time slot called Grouping Slot Time (GST) by an order specified by the AP.

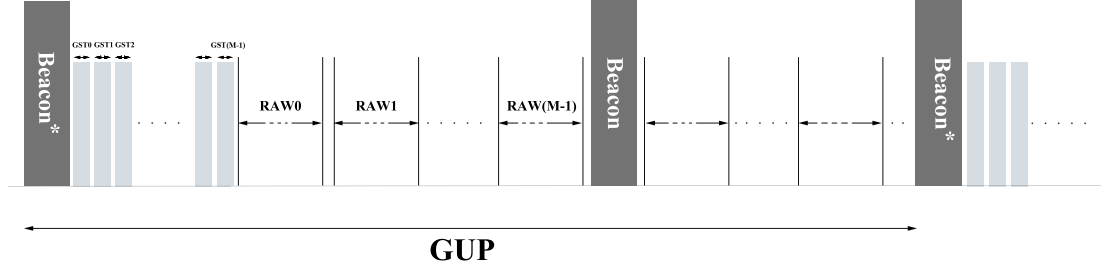**for** Each GUP **do**

   AP chooses M random nodes (group heads)

Figure 3.2: Time diagram of RSS-based grouping algorithm, Beacon* is a BF initiating the grouping scheme. As it is shown in the figure, a GUP can be as large as several beacon intervals. Essentially it can last as long as the AP is satisfied with the throughput performance.

AP informs group heads about their index in BF
AP includes M in BF
for Each node **do**
  if It is a group head **then**
    Transmits a pilot in its own GST
  else
    Measure power of each GST
  end if
end for
At the end of last GST
for Each node **do**
  if It is a group head **then**
    Joins the group with its GST index
  else
    Joins the Group with the largest power GST index
  end if
end for
end for

A time diagram of the algorithm is illustrated in Fig. 3.2 and an example of Voronoi cells is shown in Fig. 3.3.

Groups are formed in Voronoi cells around group heads. Nodes will then remain in their selected RAW until another trigger from the AP. Comparing to centralized schemes studied in [**?**] which want the AP to assign each node to a group, this scheme
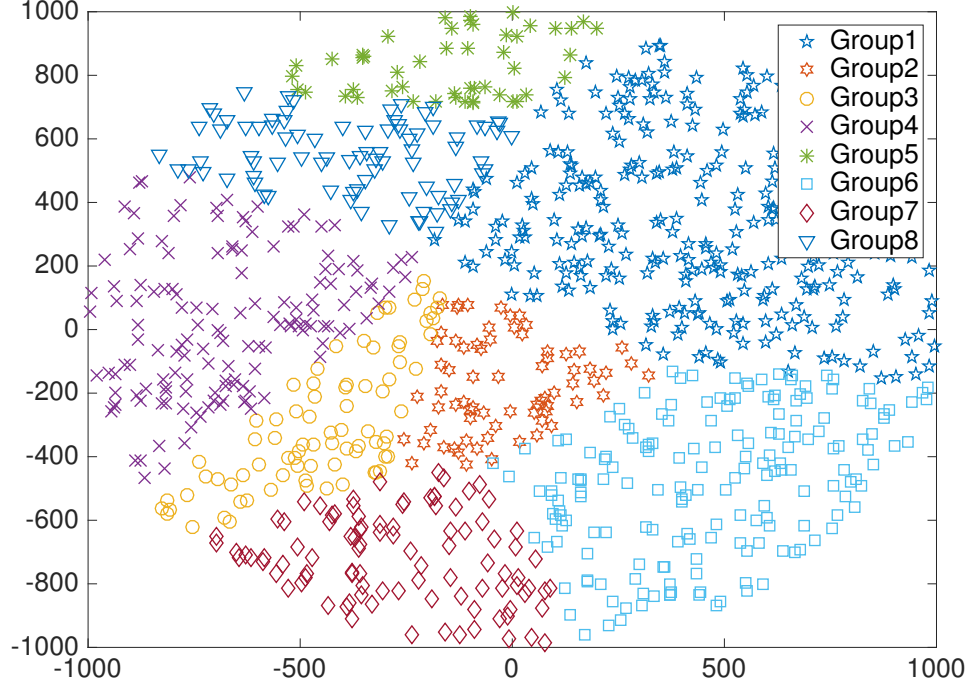
Figure 3.3: A sample grouping showing how nodes are categorized location-wise using RSS-based grouping

has a much lower control overhead and it does not require any location information to be collected and exchanged in the network.

In the rare case that a node is very far from all the group heads, which means that it can not have any measurement for any GST, it will randomly choose one of the groups.

3.4.4 Implementation Issues

The proposed scheme can be readily implemented in current IEEE 802.11 systems without any major modifications. The power measurement already exists in the MAC layer of all systems and they can provide RSSI at any time, so nodes can then find the sensed power of each GST transmission by measuring the average RSSI during the reception time of the pilot.

GST can be as small as an ACK time and there should be some guard distance time between pilot transmissions from group heads. For the best performance, the optimum value of GUP and GST should be determined which is beyond the scope of

this paper and they do not affect our following analysis. The grouping can also be triggered by the AP if the randomly selected headers result in unsatisfactory network performance.

Including M in BF is something that is already being done in the IEEE standard draft [**?**]. Informing group heads about their index can also be done using a mapping strategy similar to the one used for delivery traffic indication known as DTIM.

Our algorithm is also robust against interference from other APs. Since the GSTs are short and they could be transmitted consecutively with a gap of SIFS, any other CSMA/CA based station, e.g. other APs, cannot transmit anything during the grouping procedure.

3.4.5   Analytical Model

In order to compare the performance of grouping schemes on hidden-terminal probability, here we define two metrics and use them along with the probability of having a hidden terminal in a group to show the benefits and costs of each grouping scheme. The first metric is the average distance between nodes in a group, D_m, which is defined as

$$D_m = \frac{\sum_i \sum_{j \neq i} d_{ij}}{\binom{n_m}{2}}, \qquad \forall i \text{ and } j \in \text{group } m, \tag{3.3}$$

where n_m is the number of nodes in group m and d_{ij} is the distance between nodes i and j.

The second metric is the standard deviation of the number of nodes in different groups which specifies how evenly nodes are distributed between different groups.

$$\sigma = \sqrt{\frac{1}{M} \sum_{m=0}^{M-1} \left(n_m - \frac{N}{M} \right)^2}, \tag{3.4}$$

where N is the total number of nodes and M is the number of available groups.

The next step is finding the probability of encountering the hidden terminal problem for different schemes. The number of group head nodes in our proposed strategy is fixed so their locations follow Binomial Point Process (BPP) and there are M of them in the entire coverage area. Thus, the probability that there are k group heads

in an area of size B can be found as

$$Pr[N(B) = k | N(A) = M] = \binom{M}{k} \left(\frac{B}{A}\right)^k \left(1 - \frac{B}{A}\right)^{M-k}, \qquad (3.5)$$

where $A = \pi R^2$ is total area of network. We use D to denote the distance between one node and its nearest group head. Every node will find its nearest group head, therefore for the CDF of D we have

$$F_D(x) = 1 - Pr[N(S(x)) = 0 | N(A) = M] \quad x \geq 0, \qquad (3.6)$$

where $S(x)$ is the overlapping area between a circle centered at the observed node with radius x and the coverage area. In general $S(x) \leq \pi x^2$ and the inequality happens for nodes close to the coverage area's border. We define $\hat{F_D}(x)$ by

$$\hat{F_D}(x) = 1 - Pr[N(\pi x^2) = 0 | N(A) = M] \quad 0 \leq x \leq R. \qquad (3.7)$$

It is always true that $\hat{F_D}(x) \geq F_D(x)$ for $0 \leq x \leq R$. However, when M is large enough, which is typically the case in practice [?] the group size is so small comparing with the whole network area that the difference between $F_D(x)$ and $\hat{F_D}(x)$ becomes negligible. We use the latter as an upper-bound of the real case.

$$F_D(x) \approx \hat{F_D}(x) = 1 - Pr[N(\pi x^2) = 0 | N(A) = M]$$
$$= 1 - \binom{M}{0} \left(\frac{\pi x^2}{A}\right)^0 \left(1 - \frac{\pi x^2}{A}\right)^M \qquad (3.8)$$
$$= 1 - \left(1 - \frac{\pi x^2}{A}\right)^M \quad 0 \leq x \leq R.$$

The validity of this approximation is then verified by simulation in Section **??**.

We can find PDF of D by taking derivative of its CDF:

$$f_D(x) = \frac{2\pi M x}{A} (1 - \frac{\pi x^2}{A})^{M-1} \quad 0 \leq x \leq R. \qquad (3.9)$$

Using this PDF we can find the probability of having a hidden terminal when our RSS-based grouping scheme is used.

Figure 3.4 shows a group head and a random node called node 1 in the same group in distance X where X follows the PDF in (3.9). The circle C1 shows the sensing
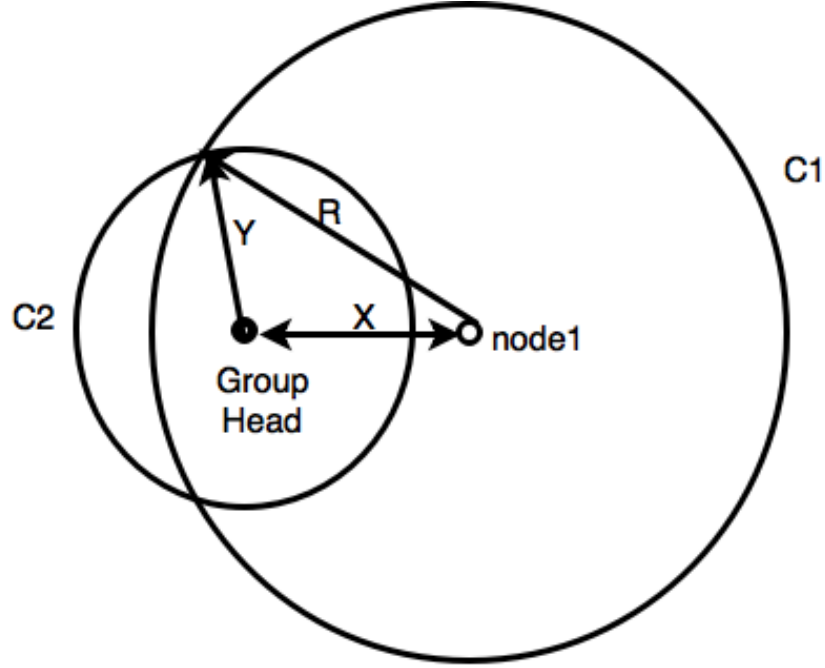
Figure 3.4: Two nodes and group head in one Voronoi cell

range of node 1 and C2 is a circle centered by the group head with the raduis Y which also follows the PDF in (3.9). The probability for node 2 which is Y away from the group head to be in the sensing range of node 1 is the ratio of the portion of C2 inside C1 to the perimeter of C2. Then, we can take the average over the PDF of X and Y to obtain the probability that two nodes are within each other's sensing range.

$$Pr_{\text{sense}} =$$

$$\int_0^{\sqrt{\frac{A}{\pi}}} \int_0^{\sqrt{\frac{A}{\pi}}} \frac{g_1(x,y)}{2\pi y} f_X(x) f_Y(y) dx dy, \tag{3.10}$$

where Pr_{sense} is the probability that two nodes in the same group are in each other's sensing range, R_s is the sensing range of a node,

$$g_1(x,y) = \begin{cases} 2\pi y & R_s \geq x + y \\ 2y \arccos(\frac{x^2+y^2-R_s^2}{2xy}) & R_s < x + y \\ 0 & R_s < |x - y| \end{cases}, \tag{3.11}$$

and $f_X(x)$ and $f_Y(y)$ are the PDF of X and Y respectively.

We can also derive the same probability for random grouping schemes. The probability density function for the distance between two random nodes in a circle with the radius R is given in [?]

$$f(r) = \frac{2r}{R^2} \left(\frac{2}{\pi} \arccos(\frac{r}{2R}) - \frac{r}{\pi R} \sqrt{1 - \frac{r^2}{4R^2}} \right), \quad 0 < r < 2R. \tag{3.12}$$

In this case, for random grouping, the probability of that two nodes in the same group are in each other's sensing region can be obtained as follows,

$$Pr_{\text{sense}} = \int_0^{2R} g_2(r) f(r) dr, \tag{3.13}$$

where

$$g_2(r) = \begin{cases} 1 & r \leq R_s \\ 0 & r > R_s \end{cases}. \tag{3.14}$$

These probabilities can then be calculated by numerical methods.

Chapter 4

Multi-Hop Transmission

4.1   Physical Layer Network Coding

Here , explain the main idea of pnc.

4.2   Implementation

We implemented the proposed MPNC on USRP and GNURadio to build the multi-hop wireless testbed. For MPNC, the transmitter and receiver in the single-hop transmission can be made using regular transmission and reception chains. In this work, standard BPSK blocks of GNURadio are used for all steps of communication, modulation, timing recovery, phase tracking and demodulation.

For MA transmissions, signals from two transmitters are synchronized in the symbol level. The synchronization issue has been heavily investigated, e.g., SourceSync [**?**] can achieve low-overhead distributed synchronization with the accuracy of tens of ns, smaller than the symbol duration (e.g., 802.11 OFDM symbol time of 4 μs). As synchronization for a static TDMA network is relatively easy and it in fact makes the estimation and compensation of CFOs and detection of preamble during the MA transmission more difficult, we use a MIMO cable to synchronize the transmitters in our USRP testbed, and focus on the most challenging part, the receiver of MA transmission with symbol level synchronization.

4.2.1 Signal formulation

Since the oscillator at the mixer of practical devices is never perfect, the real carrier frequency of each device may be slightly different from the nominal value. This causes a small rotating phase to remain in the signal after the mixer. In regular point-to-point communications, this frequency offset can be estimated and compensated using phase tracking algorithms. The same algorithms are no longer useful in MA transmissions since the signals are from two sources and there are two frequency offsets, so the resulting phase cannot be removed by a simple multiplication. Several algorithms have been proposed [?, ?, ?, ?] to compensate the effect of CFO when multiple signals are mixed at the receiver. These algorithms either require a small portion of interference-free part in two signals, which are not directly applicable for MPNC with symbol level synchronization. Another approach is to use the mean of two frequency offsets to partially compensate the frequency offsets for PNC MA transmission [?]. In multi-hop scenarios, error propagation is a severer problem than that in the two-hop PNC case, so a careful design that can accurately compensate the two CFOs is needed.

Assuming that nodes A and B are transmitting symbol a_k and b_k at the k_{th} symbol interval, respectively, the baseband signal can be written as

$$x(t) \;=\; \sum_{k=0}^{k=N} a_k g(t - kT), \quad \text{and} \tag{4.1}$$

$$y(t) \;=\; \sum_{k=0}^{k=N} b_k g(t - kT), \tag{4.2}$$

respectively, where $g(t)$ is the pulse for the pulse shaping step (a root raised cosine (RRC) pulse is used here), N is the number of symbols in one packet, and T is the symbol interval. Considering the received signal as

$$r(t) = x(t - \tau)H_a e^{j2\pi(f_a)t} + y(t - \tau)H_b e^{j2\pi(f_b)t}, \tag{4.3}$$

where f_a (f_b) is the CFOs between the oscillator of the receiver and that of A (B), respectively, and τ is the time delay. In the MA transmission, f_a and f_b can be estimated at the beginning of each packet. Considering the wireless channels to be frequency flat and constant during the reception time of a packet, H_a (H_b) can be represented with one tap, essentially a complex number. The received signal after the

Analog to Digital Converter (DAC) is given by

$$r_n = h_1 x e^{j\omega_1 n + \phi_1} + h_2 y e^{j\omega_2 n + \phi_2}, \qquad (4.4)$$

where h_i, ϕ_i, and ω_i, $i = 1, 2$ are the gains, phases and digital frequency offsets imposed by the channel and the receiver circuit, respectively.

4.2.2   Timing recovery

Depending on the sampling rate of the Digital to Analog Converter(DAC), each symbol is represented with a constant number of samples. This parameter is called Samples per Symbol (SpS) and can be found as Tf_s, where f_s is the sample rate of the DAC. After passing the received signal from the matched filter, the next step is to down sample the signal to one sample per symbol before detection.

In the digital domain, depending on the offset between the transmitter and receiver's clocks, only one of the samples representing a symbol is used for detection and the distance between valid samples is equal to SpS. As shown in Fig. 4.1, to find the valid sample, the signal is divided into different branches and decimated with different time delays, from 0 to $SpS - 1$. The signal after downsampling can be expressed as

$$s_k = h_1 a_k e^{j(SpS)\omega_1 n + \phi_1} + h_2 b_k e^{j(SpS)\omega_2 n + \phi_2}. \qquad (4.5)$$

Each branch is then used for preamble detection purposes and the result is connected to a switch. The same preamble detection algorithm is ran for all branches. If a preamble is identified, the signal would be annotated with a tag consisting of ϕ_i and ω_i ($i = 1, 2$). The switch then copies only the branch with a tag to output. It is possible to find a preamble in more than one branch. The preamble detector block also includes the mean square error of detection so the switch can choose the branch with the best signal to noise ratio.

4.2.3   MA receiver, CFO estimation

To help the receiver estimate CFOs and detect MA transmissions, each frame begins with a Sync preamble and a start of frame delimiter (SFD) part. The sync preamble is a series of zeros and ones, and the SFD is used to verify the detection of a packet. In our work, the Sync preambles for node A and B are "1010... 10" and "0101...01",
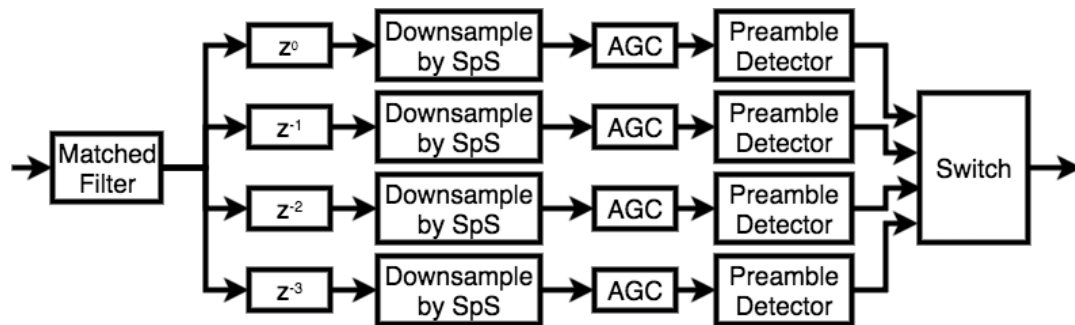
Figure 4.1: Receiver chain.

respectively, which is similar to the packet structure used in the IEEE 802.11 FH PHY.

Before using the signal to detect a preamble, the signal is passed from an Automatic Gain Control (AGC) unit, in order to normalize the channel gains, h_1 and h_2. In a window with a large enough number of symbols, there exists at least one instant that symbols from both sources has an equal or very close phase and have been added constructively. So the AGC adjusts the maximum absolute value of symbols to two. For BPSK, +1 and -1 represents 1 and 0, respectively. If we index all symbols of the sync part starting from 0, the k_{th} received symbols of Sync preamble can be written as

$$s_k = (-1)^{k+1} e^{p_{1,k}} - (-1)^k e^{p_{2,k}}. \tag{4.6}$$

For consistency, we replace all odd indexed symbols of Sync with their additive inverse so the k_{th} symbol can be represented as

$$s'_k = e^{p_{1,k}} - e^{p_{2,k}}. \tag{4.7}$$

The two phases of $p_{1,k}$ and $p_{2,k}$ can be found by solving the equations below

$$\begin{cases} Re(s'_k) = \cos(p_{1,k}) - \cos(p_{2,k}), \\ Im(s'_k) = \sin(p_{1,k}) - \sin(p_{2,k}). \end{cases} \tag{4.8}$$

Since there may be multiple possible answers for these equations, $p_{1,k}$ and $p_{2,k}$ are chosen in a way that they are closest to $p_{1,k-1}$ and $p_{2,k-1}$ and increasing or decreasing linearly.

The frequency and phase offsets are then found by a solving a linear regression according to the following equations,

$$\begin{cases} p_{1,k} = (SpS)\omega_1 k + \phi_1, \\ p_{2,k} = (SpS)\omega_2 k + \phi_2. \end{cases} \tag{4.9}$$

4.2.4 MA receiver, preamble detection

A window with the length of the Sync preamble is always sliding on the received samples. Then each time the above CFO estimation algorithm is applied and the ϕ_i and ω_i ($i = 1, 2$) are used to decode the next L_{SFD} symbols of the packet where L_{SFD} is the length of the SFD part. If the decoded SFD matches the expected SFD, which

is XOR of SFD of node A and node B, then the packet is detected and the rest of the symbols are decoded using the same parameters. In our design, SFDs by nodes A and B are "1010 0110 1101 0110" and "1010 1010 0110 1011", respectively, so the SFD expected in the relay is "0000 1100 1011 1101".

Because of the presence of CFO and phase offset, the constellation is changing from one symbol to another. The right constellation for each received symbol is calculated using the ϕ_i, and ω_i and then used for decoding and mapping, as shown in Fig. **??**.

Chapter 5

Experiments, Evaluation and Comparisons

talk in general about the evaluation, methods used and explain what's comming in next sections

5.1   rss - based evaluations

The performance of different grouping schemes is evaluated using MATLAB and NS-2[?]. MATLAB is used for numerical calculations and NS-2 is used for throughput simulations. The network coverage is assumed to be a circle with radius 1 km which is the case in sub 1GHz network having the access point at the center. As mentioned in Section 3.4.2, nodes are uniformly placed in the coverage area with their number following a Poisson distribution with density 0.0019 node per square meter which results in 6000 nodes in the network on average. The number of groups, M, was set in the range of 8 to 512. For each setting, the experiments were repeated 20 times, and the average was taken.

If the AP the knows location information of all the nodes, in a pure centralized solution where AP decides the group for each node, the k-means algorithm can be used to achieve near-optimal groupings. So we can use the performance with k-means grouping as a benchmark to see how well our RSS-based distributed grouping algorithm is working compared with the centralized benchmark.

In Fig. 5.1a, the average distance between nodes in a group for the proposed scheme is always smaller than with the random grouping scheme and close to the

(a) Average D_m over all groups

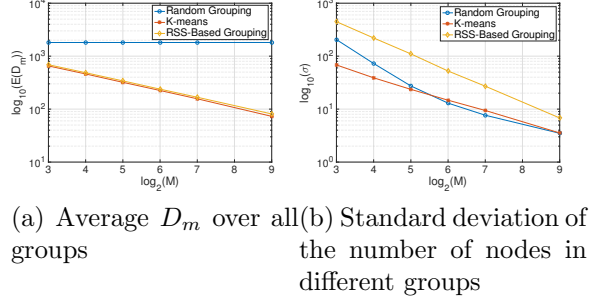(b) Standard deviation of the number of nodes in different groups

Figure 5.1: Grouping performance metrics

k-means clustering algorithm. It is also obvious that a larger number of groups have a smaller average distance between nodes for all algorithms.

In Fig. 5.1b, we can see that the standard deviation of the number of nodes in different groups is the cost that the RSS-based grouping algorithm pays for the advantage of distributed solution. Groups with a large number of users will suffer from high collision probability and groups with a very small number of users may not fully utilize their RAW. It is shown later using NS-2 simulations, that despite having some dense groups, the RSS-based grouping algorithm has a better performance than random groupings. This is because the hidden node problem is a more severe problem than uneven groups. A few hidden terminals can dramatically decrease the performance of the whole network. Having more nodes that are all in the sensing range increases the competition but has a less destructive effect on the throughput than that due to hidden terminal.

Assuming that all nodes have the same sensing range, R_s, the probability of two random nodes in the same group be in their sensing range versus R_s for a constant number of groups is shown in Fig. 5.2a. The figure also shows that the approximation in (3.8) not affect the result very much. As we can see in the figure, best performance is for the clustering using the k-means algorithm but the RSS-based grouping scheme also performs very close to the k-means and much better than the random grouping schemes. The same probability assuming Rayleigh fading channel between nodes is also shown in Fig. 5.2a. The performance with Rayleigh fading channels is degraded because considering fast fading the areas occupied by groups are no longer Voronoi and the group head with the highest sensed power is not necessarily the closest one. As shown in the figure the algorithm still performs well which indicates that, the RSS estimation accuracy required is low, which results in a small overhead.
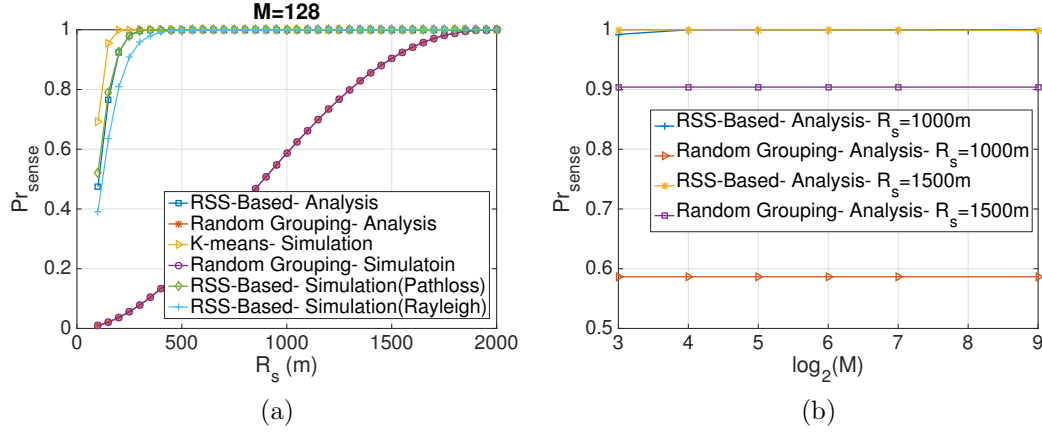
Figure 5.2: Probability of two nodes, within a group, being in the sensing range of each other

With the simulation results following analytical results, our assumption in section **??** is verified. The simulation and analytical results are closer to each other as M grows. That is because, with a higher value of M, the edge effect becomes more negligible.

Fig. 5.2b shows the probability of two nodes in the same group being in each other's sensing range when all nodes' sensing range is fixed and the number of groups changes. This probability does not change with the number of groups for random grouping because nodes in the same group can still be anywhere in the coverage area and their distance still follows the same PDF. Though in case of the RSS-based grouping algorithm, a larger number of groups results in a higher probability for group members to be in the sensing range of each other because it makes the Voronoi cells smaller.

Fig. 5.8 shows the throughput simulation result for different grouping schemes along with k-means clustering algorithm using NS-2. Table 5.1 shows the parameter setting for simulations used in this section. Other common settings such as PHY and MAC header are set according to the IEEE 802.11 standard [**?**]. The payload size is set to be low considering the IoT applications such as smart meter measurement reporting and all nodes are using RTS/CTS mechanism. Only the uplink traffic is considered and a non-collided transmission is assumed to be successful which that means the PHY layer BER is not considered.

In Fig. 5.8, the throughput for random scheme is very low because the time for a single packet transmission is more than the largest back off window (1024 slots)
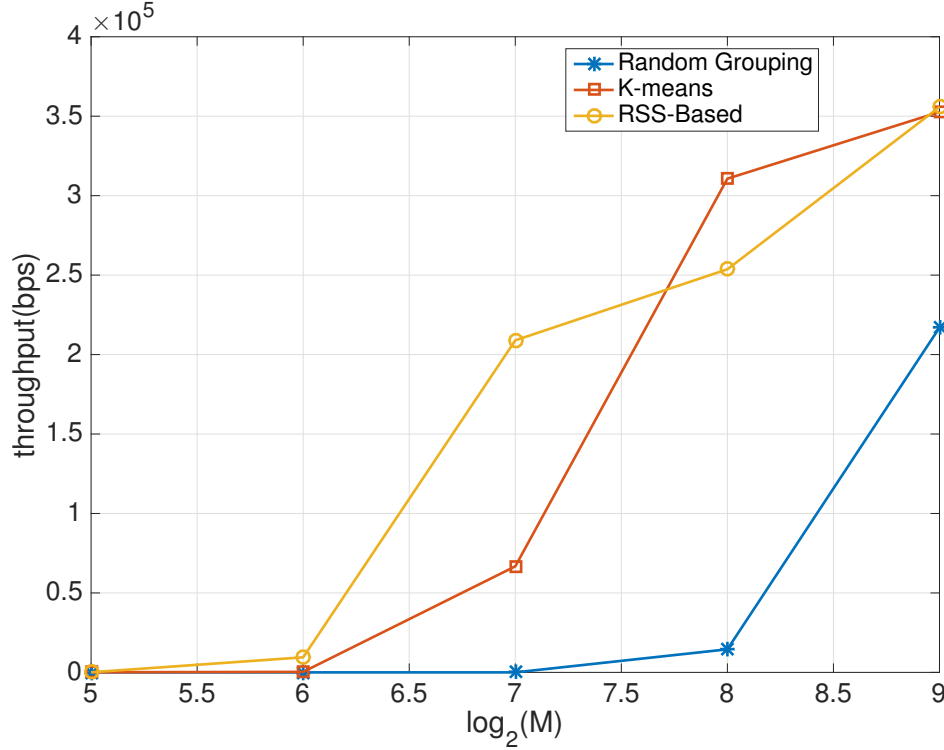
Figure 5.3: Throughput of Uplink traffic

and almost any transmission would be interrupted when there is a few active nodes who are hidden terminals. In other words, a node with a hidden terminal may hardly success in transmitting a packet to the AP without collision.

This figure also shows the limited cost that RSS-based grouping pays due to the higher standard deviation of number of nodes in each group. The throughput using the proposed RSS-based grouping is close to that using the centralized K-mean solution. On the other hand, random grouping has much worse performance due to the hidden terminal problem even when the sensing range is as high as 1500m. Note that the theoretical sensing range without considering the shadowing effect may be much higher than the practical sensing range, so grouping considering the location is important to avoid hidden terminal and improve network performance.

5.2 PNC evaluations

a section to discuss resutls of pnc impelemntation

Table 5.1: Throughput Simulation Parameter Setting

Parameter	Value
Slot time	20 μS
SIFS	10 μS
Payload Size	64 bytes
Data Rate	1Mbps
R_s	1500
CW min	31
CW max	1023

5.2.1 Testbed Experiments

Experiment setting

USRP N210 sets with XCVR2450 daughterboards are used to run the MPNC experiments. The software used to develop MPNC is GNURadio. The transmission gain of transmitting USRPs is set to 18 dB and the receiver gain of receiving USRPs is set to 5 dB. The carrier frequency is chosen as 2.45 GHz. The length of the Sync preamble is 64 symbols and the SpS used in the experiments is four.

5.2.2 BER, two-hop

To begin with, we first built a two-hop testbed where two sources A and B exchange the information through a relay, as shown in Fig. 5.4.

Fig. 5.5 (a) and (b) shows the BER in the MA communications and the end-to-end BER for the two-hop case, respectively. As anticipated, the BER performance deteriorates when the payload length increases, due to the non-stationary wireless channel and the CFOs. Thus, to maintain a low BER, preambles could be repeated periodically. A somewhat surprising resul in Fig. 5.5 (a) is that there is a small drop of BER around 150-bit block length. This is because, due to CFO, the phase difference of the two transmissions superimposed at the relay changes periodically. From Sec. **??**, BER with different phase shift is slightly different. After 100-bit was sent, the phase shift returns to the area corresponding to low BER.

The end-to-end BER results in Fig. 5.5 (b) include both the MA transmissions and the broadcast transmissions from the relay to the sources. We further compared the end-to-end BER performance of PNC with that of ANC reported in [**?**]. The relay in ANC uses an amplify-and-forward approach, instead of the mapping function. From
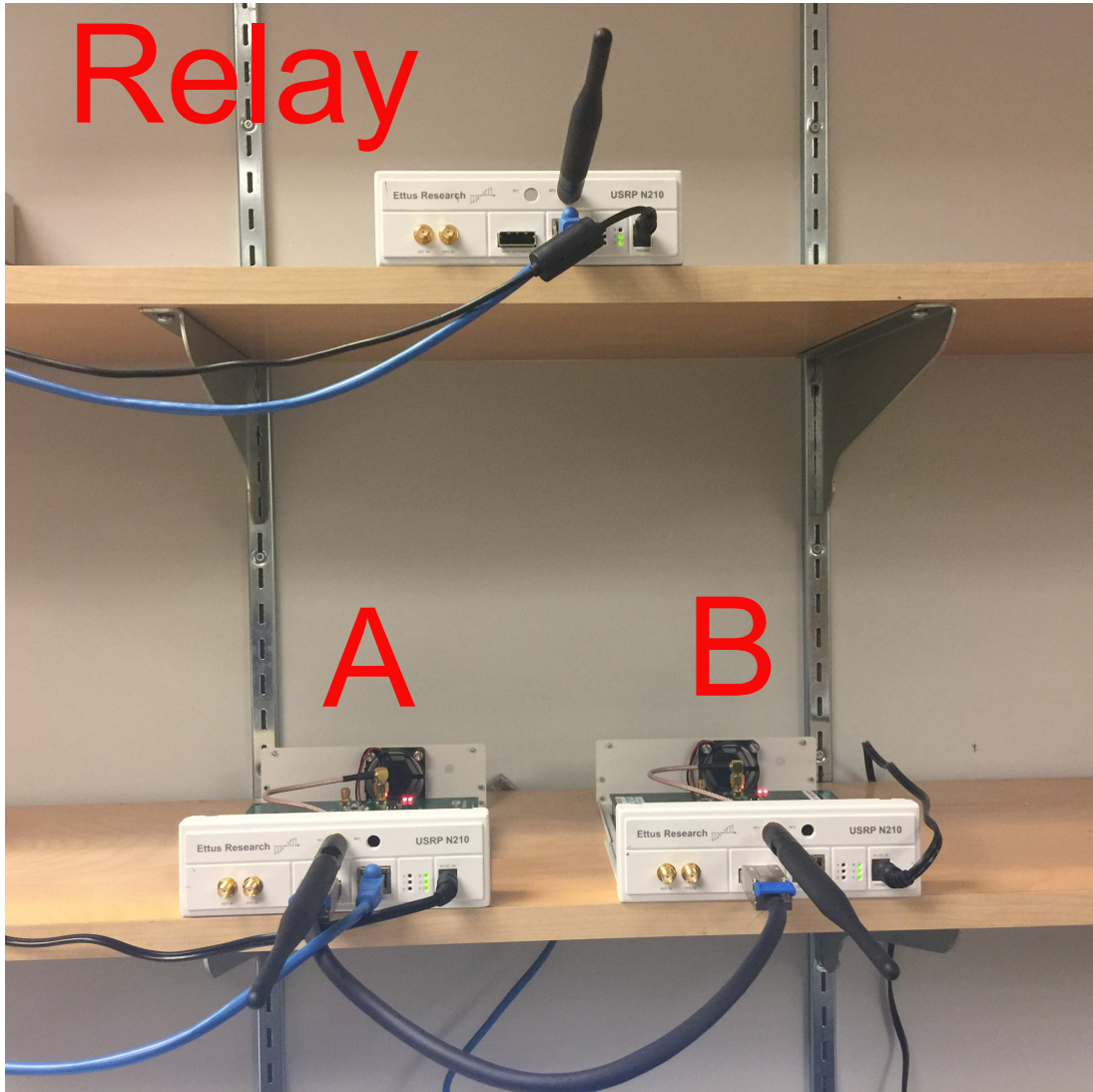
Figure 5.4: Testbed, two-hop scenario.

(a) MA transmission BER   (b) End-to-end BER   (c) MPNC vs. ANC
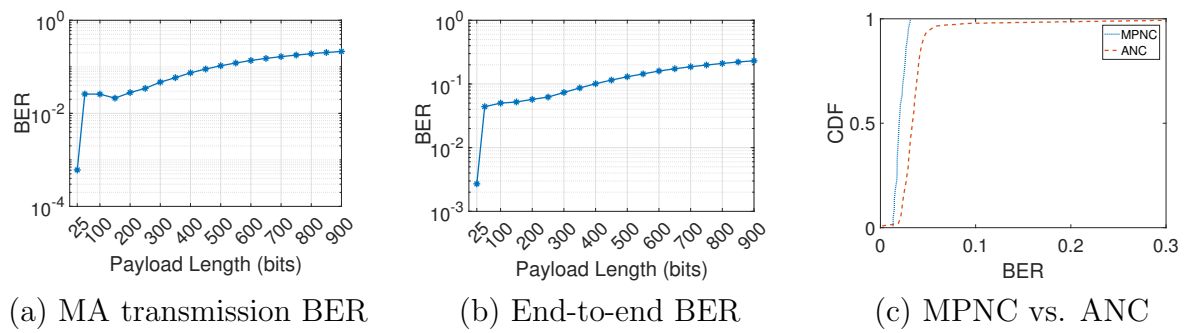
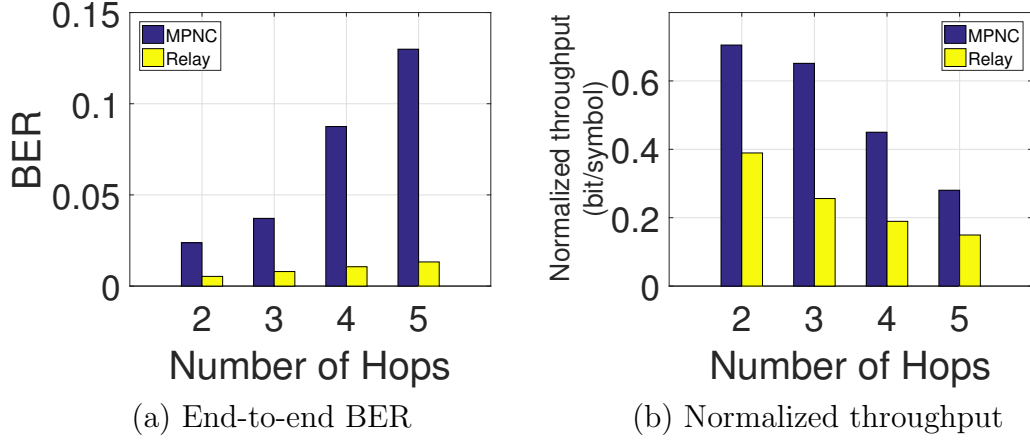Figure 5.5: BER performance, two-hop.

Figure 5.6: Multi-hop performance.

Fig. 5.5 (c), MPNC slightly outperforms ANC, from the USRP testbed experiments. In general, the performance of amplify-and-forward degrades in the low SINR region.

Multi-hop performance

Next, we extended the two-hop scenario to multi-hop scenario, where the number of hops varied from two to five. The transmission and reception of the relays for multiple hops behave similarly as that in the two-hop case, except that the mutual interference and the error propagation problem will lead to a higher BER.

Figs. 5.6 (a) and (b) compare the end-to-end BER and normalized throughput, respectively of MPNC and that with hop-by-hop relay. The normalized throughput is the number of bits successfully received by the destination per symbol duration. From the figures, although the end-to-end BER of MPNC is much higher than that of hop-by-hop relaying, due to both the worse BER performance in MA transmissions and the error propagation problem (i.e., a single MA transmission error may affect multiple end-to-end bit errors in a multi-relay path), the end-to-end throughput of MPNC is much higher than that of hop-by-hop relay. Using the inexpensive USRP testbed, it is encouraging to notice that the performance gain of MPNC ranges from 75% to 80% for the two- and five-hop cases, and around 150% for the three- and four-hop cases.
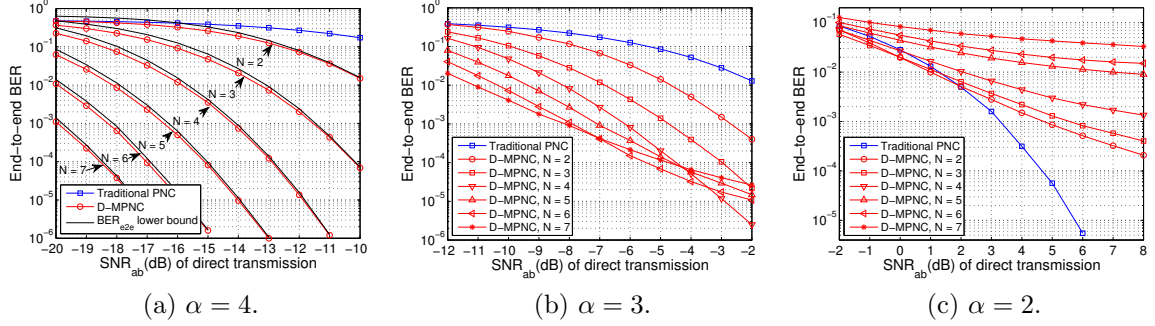
Figure 5.7: End-to-end BER performance of MPNC under AWGN channel.

5.2.3 Simulation Results

To evaluate and compare the performance of the proposed MPNC in controllable and repeatable environment with a wide range of settings, we used Matlab and GNURadio to conduct extensive simulations and the results are presented in this section.

Different number of hops

In this subsection, we study the end-to-end performance considering different number of hops, aiming to identify the optimal number of hops. For fair comparison, here, we let the total transmission power in any two continuous slots be $2E_b$, and all the nodes equally share the total transmission power. In other words, if the number of hops increases, the transmission power per node decreases accordingly. The nodes are located in a linear topology with equal distance for each hop. The average received SNR of all links are proportional to $d^{-\alpha}$, where d is the hop distance.

Since the end-to-end data exchange rate of PNC and MPNC remains the same no matter how many relays are used, we only need to compare the end-to-end BER performance. The end-to-end BER results considering different number of relays and different path loss exponents are shown in Fig. 5.7. The X axis is the end-to-end SNR_{ab}(dB) by direct transmission (without any relay). The "Traditional PNC" curves are for the case with one relay only so the traditional PNC solution can be directly applied. With N relay(s), the transmission power per node is less while the path loss also reduces. The mutual interference also increases when the number of relays increase. Therefore, there is a tradeoff, and the optimal number of hops largely depends on α, typically ranging from 2 to 6 [?].

In Fig. 5.7(a), the black curves are the end-to-end BER bound of MPNC obtained

in Table **??** and the red circled curves are the simulation results. When the BER is low, the bound and the simulation results converge. This is because, when the BER is low, the probability that more than one multi-access and single-hop errors occur in a slot becomes negligible. Comparing Figs. 5.7(a), (b) and (c), α has a great impact on the end-to-end BER performance. In Fig. 5.7(a), when $\alpha = 4$, MPNC outperforms the traditional PNC with single relay significantly due to the a relatively larger SINR between the neighbor nodes as the interference and signal strength both decay fast with distance. The tendency also shows that with the lower end-to-end SNR (or larger distance between the sources), we can add more relays to ensure that the BER is below a threshold. In Fig. 5.7(c), when $\alpha = 2$, the two-hop PNC achieves the best performance when the end-to-end SNR is above 2 dB; and below that, all solutions perform poorly. In Fig. 5.7(b), when $\alpha = 3$, the optimal number of relays depends on the end-to-end SNR (or distance). The results suggest that when α is large (e.g., ≥ 3), we can apply MPNC to solve long-distance wireless transmissions using a large number of relay.

Goodput performance comparison

In this section, the goodput of MPNC is studied and also compared with the other state-of-the-art solutions. As we compare the performance of different solutions with the same number of hops, different from the last subsection, here, the transmission power of each node and the hop distance remains constant. The goodput measures the number of error-free packets received per slot. For the full-duplex relay solution, in the simulation, we made a strong assumption that the self-interference can be fully cancelled. Thus, the performance shown in our simulation can be viewed as the upper bound of it. As the existing PNC method for multi-relay path suffers from the infinite error propagation problem, to make it usable, after detecting each error, the destination must notify all other nodes and the pipeline should be flushed and restarted. The goodput for the PNC method is thus affected by the restarts. Note that with the infinite error propagation problem, an error detection coding have to be used for PNC, but the error correction coding cannot be applied, which is a severe disadvantage for it.

The goodputs are shown in Fig. 5.8. Comparing with the other state-of-the-art algorithms, MPNC has always a higher goodput and can maintain its performance as the number of hops increases. The goodput gains of MPNC over hop-by-hop relay,
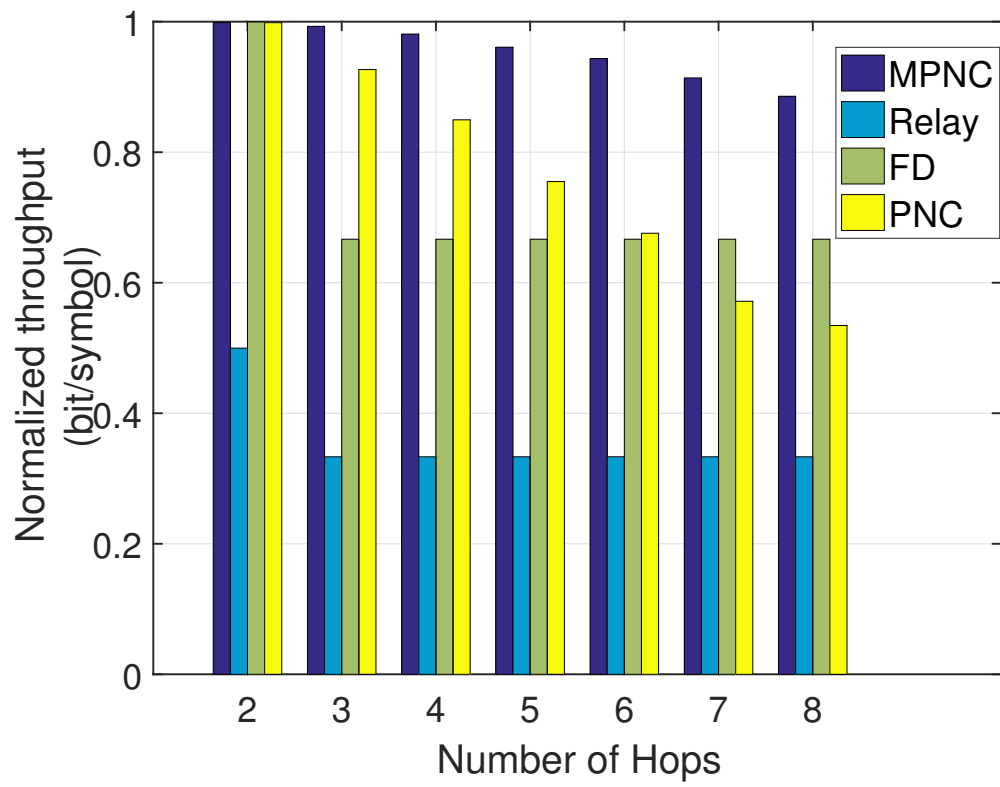
Figure 5.8: Goodput, per-hop SNR = 9, $\alpha = 4$, Payload=256 bits.

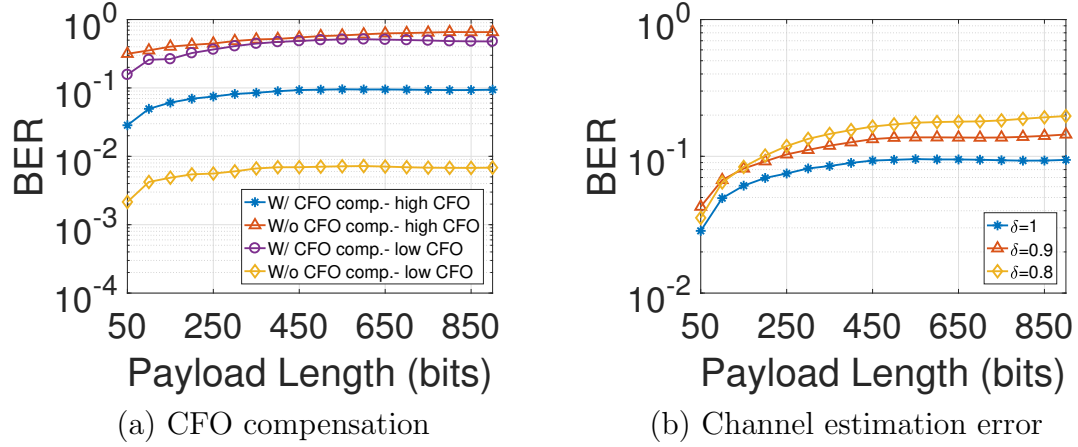(a) CFO compensation   (b) Channel estimation error

Figure 5.9: Effect of CFO and channel estimation error on BER.

full-duplex, and PNC is about 3x times, 33%, and 68% when the number of hops is as high as eight. Also, from the figure, the goodput of MPNC remains close to 0.9 packet/slot when the number of hops varied from two to eight, showing that it is quite scalable to long paths.

Effect of CFO on BER

Fig. 5.9 (a) shows the impacts of CFOs on the BER performance. High CFO is set according to the practical number measured from the USRP devices in our testbed, and the low CFO is 0.1 of that. As it can be seen in the figure, CFO compensation is crucial to the performance of MPNC. The figure shows that when CFO is not compensated, the performance is poor (larger than 10% bits in error) no matter whether the CFO is high or low. On the other hand, using the proposed CFO compensation algorithm can improve the BER performance significantly.

Effect of Channel Estimation Error on BER

We studied the effect of channel estimation error on end-to-end BER performance. In Fig. 5.9 (b), δ represents the ratio of estimated channel gain and the real channel gain. From the figure, overall, the BER increases when the channel estimation error increases, while the algorithm can maintain a reasonable BER even with 10% to 20% estimation errors.

Chapter 6

Conclusions

talks conclusions stuff. here is the conclusion of the grouping manuscript: The hidden terminal problem under GS-DCF has been addressed in this paper. An RSS-based grouping scheme has been proposed. The proposed scheme will categorize users in RSS-based groups so nodes in the same group can be close enough that the probability of having a hidden terminal is very low. The performance of RSS-based grouping has been then studied and compared to random and optimal grouping schemes using analytical and simulation results presenting different metrics.

Another problem in future infrastructure networks that can be solved with RSS-based groups is small message size of most sensing data exchanges, which will reduce channel efficiency. [?] showed that small packet size will reduce the overall throughput. RSS-based grouping schemes can easily utilize clustering algorithms where each group is a cluster and a cluster head in each group can act as a relay for other nodes. We intend to cover this application in our future work.

Bibliography

[1] Cliff Atkinson. *Beyond Bullet Points: Using Microsoft Office PowerPoint 2007 to Create Presentations That Inform.* Microsoft Press, 2008.

[2] Wayne Booth. *The Craft of Research.* University of Chicago Press, 2003.